

Unified hydrodynamic approach to laser field plasmon excitations in metal nanoparticles with general shape

S. V. Fomichev*

*National Research Center "Kurchatov Institute," 1 Kurchatov place, 123182 Moscow, Russia and
Moscow Institute of Physics and Technology, 141700 Dolgoprudny, Moscow Region, Russia*

A. M. Bratkovsky†

*Hewlett Packard Laboratories, 1501 Page Mill Road, Palo Alto, California 94304 and
P. L. Kapitza Institute for Physical Problems, 2 Kosygina Str., 119334 Moscow, Russia*
(Received 12 October 2012; revised manuscript received 24 May 2013; published 22 July 2013)

We present a unified hydroelectrodynamical approach to study electron dynamics in a laser field in cold metal nanoparticles with a general nonspherical surface. This is the generalization to complex shapes of the model used earlier to study both linear and nonlinear plasmon excitations in thin metal films and spherical nanoparticles. Along with a general formulation allowing a direct nonlinear extension of the model for nanoparticles with nonspherical shapes, the linear plasmon excitations in metal cubic and rectangular parallelepiped nanoparticles are calculated as an example of using the hydrodynamic model in a cold charge-compensated electron plasma approximation. The results obtained for the cubic and parallelepipedlike nanoparticles are analyzed and compared with the ones of earlier approaches such as the discrete dipole approximation.

DOI: [10.1103/PhysRevB.88.045433](https://doi.org/10.1103/PhysRevB.88.045433)

PACS number(s): 36.40.Gk, 42.65.Ky, 52.38.Dx, 73.22.Lp

I. INTRODUCTION

Collective electron excitations in metal nanoparticles (plasmons) play an important role in physics, material science, biology, nanoelectronics, and numerous applications.¹ The dipole (i.e., the strongest) resonance at some frequency ω_d that is usually quite different from the bulk plasmon frequency of the metal ω_p can be excited by a laser beam with frequency $\omega \approx \omega_d$ in the linear regime with respect to the laser intensity. The classical plasmon (the Mie resonance at $\omega_d = \omega_p/\sqrt{3}$) corresponds to a giant dipole resonance, where the conduction electrons oscillate in unison in spherical metal particle in vacuum like an incompressible charged fluid confined by the positive potential of ion core. In nonspherical (or, more specifically, in nonellipsoidal nanoparticles) the incompressibility approximation of the charged fluid is no longer supported.² Additionally, the restoring force on the electrons in nanoparticles is generally nonlinear due to the presence of a sharp particle surface, including that for the spherical one. As a result, higher harmonics can be excited, too, depending on the laser field strength. If the particle has a center of inversion (like a sphere or a cube, but not, e.g., a tetrahedron), the force would be odd with respect to inversion, so the third harmonic will be the strongest in the far field, while both odd and even harmonics will be present in the near field. One expects very strong interplay between these two effects, plasmonic resonance and nonlinear restoring force, leading to a giant enhancement of n th-order harmonic at a resonance condition $n\omega = \omega_d$, $n \geq 1$. This will generate an *extremely strong* n th-order harmonic field in the vicinity of the particle. In turn, this can be used to excite very strong Raman scattering from molecules near the particle³ very useful for sensing, or generate very high-order harmonics in extreme UV range 20–120 nm by injecting noble gas into the nanostructures with high field concentration due to plasmon excitation,⁴ and in many other applications of nonlinear plasmonics.⁵

Now, the problem for plasmon excitations in metal nanoparticles is generally considered either in a quasistatic approximation^{6,7} or in a popular discrete dipole approximation (DDA) accounting for retardation⁸ (cf. also Refs. 2, 3, 9, 10 and 11, and references therein), finite difference time domain (e.g., Ref. 12), or finite element methods (e.g., Ref. 13). In the present paper, the coupled hydrodynamic and electrodynamic approach will be developed to study the plasmon resonances in general nonspherical subwavelength nanoparticles. This is the generalization to complex shapes of the electron's hydrodynamic model developed earlier to study the linear and nonlinear plasmon excitations in thin metal films and spherical nanoparticles with diffuse surfaces.^{14,15} The method will be shown to be fast and versatile as it allows direct nonlinear expansion to treat linear and nonlinear effects in metal nanoparticles and their assemblies on equal footing that is hard to obtain in other approaches such as DDA, LDA, etc. Quite unexpectedly, however, it occurs that in order to get a closed set of hydro/electrodynamical equations even for small (subwavelength) particles of any shape including the spherical one, one needs to retain the magnetic field usually neglected in customarily used quasistatic approximation. As a first example of its applicability to particles with nonspherical shapes, we shall apply it here to study a linear electromagnetic response of the perfect cube/parallelepipedlike metal nanoparticles. In the case of a cube discussed below, it apparently brings about some differences with, e.g., standard DDA calculations even in a linear regime.² The results for nonlinear plasmon response of cubelike nanoparticles will be presented in a separate paper. Here, we would like to stress that among other things the present formalism opens up the possibility for consistent calculations of both linear and nonlinear responses in particles of practically arbitrary shape not available before. Note that prior attempts to solve nonlinear problems were usually limited to the simplest geometries such as spherical particles^{16–19} and used various crude approximations such as an incompressible

electron fluid, infinite confinement potential, etc. (see, e.g. Ref. 19, and references therein).

The paper is organized as follows. In Sec. II the unified hydrodynamic model, which permits direct expansion for calculation of both a linear and a nonlinear electromagnetic response of a nanoparticle with a general surface shape is described, along with the boundary conditions for both electric potential and magnetic field on the arbitrary surface of the nanoparticle. In Sec. III, we present first results of the calculations within our model of the linear electromagnetic response of the perfect cubelike nanoparticles as an example both in the far-field and in the near-field ranges. The rectangular parallelepipeds are also considered to discuss the results and to compare them with previous methods. Finally, Sec. IV gives a summary of the results.

II. MODEL

Consider the dynamics of the electrons of a nanoparticle starting from the collisionless hydrodynamic equations:

$$\frac{\partial n_e}{\partial t} + \text{div } \mathbf{q} = 0, \quad (1a)$$

$$\begin{aligned} \frac{\partial q_\alpha}{\partial t} + \gamma \omega_p q_\alpha + \frac{\partial (P_{\alpha\beta}/m_e + q_\alpha q_\beta/n_e)}{\partial x_\beta} + \frac{en_e}{m_e} (E_\alpha + E_\alpha^L) \\ + \frac{e}{m_e c} e_{\alpha\beta\gamma} q_\beta (H_\gamma + H_\gamma^L) = 0, \end{aligned} \quad (1b)$$

$$\begin{aligned} \frac{\partial P_{\alpha\beta}}{\partial t} + \frac{1}{n_e} (\mathbf{q} \cdot \nabla) P_{\alpha\beta} + P_{\alpha\gamma} \frac{\partial (q_\beta/n_e)}{\partial x_\gamma} + P_{\beta\gamma} \frac{\partial (q_\alpha/n_e)}{\partial x_\gamma} \\ + P_{\alpha\beta} \text{div}(\mathbf{q}/n_e) + \frac{e}{m_e c} (e_{\alpha\gamma\delta} P_{\beta\gamma} + e_{\beta\gamma\delta} P_{\alpha\gamma}) (H_\delta + H_\delta^L) \\ = 0, \end{aligned} \quad (1c)$$

with $n_e(t, \mathbf{r})$ the electron density, $\mathbf{q}(t, \mathbf{r})$ the electron flux density, and $P_{\alpha\beta}(t, \mathbf{r})$ the electron pressure tensor.²⁰ In Eqs. (1a)–(1c), m_e is the electron mass, e is the absolute value of the electron charge, c is the speed of light, $\mathbf{E}^L(t, \mathbf{r})$ and $\mathbf{H}^L(t, \mathbf{r})$ are the electric and magnetic components of the external electromagnetic field acting on electrons in the nanoparticle, and $\mathbf{E}(t, \mathbf{r})$ and $\mathbf{H}(t, \mathbf{r})$ the self-consistent electric and magnetic fields of the ions and electrons. Although the above equations can generally be obtained from the collisionless Vlasov kinetic equation,²⁰ the second (relaxation) term in Eq. (1b) with the dimensionless relaxation constant γ , which is normalized to the bulk plasma frequency $\omega_p = \sqrt{4\pi e^2 z_i n_{\text{ion}}/m_e}$, was introduced phenomenologically. Here, z_i is the mean ionic charge and n_{ion} is the reference bulk ion density of the nanoparticle substance. This collisionlike term simulates weak binary collisions. For their solution, the above hydrodynamic equations should be solved simultaneously with the Maxwell equations

$$\text{div } \mathbf{E} = 4\pi e(z_i n_i - n_e), \quad \text{div } \mathbf{H} = 0, \quad (2a)$$

$$\text{curl } \mathbf{E} = -\frac{1}{c} \frac{\partial \mathbf{H}}{\partial t}, \quad \text{curl } \mathbf{H} = \frac{1}{c} \frac{\partial \mathbf{E}}{\partial t} - \frac{4\pi e \mathbf{q}}{c}. \quad (2b)$$

In Eqs. (2a) and (2b), $n_i(\mathbf{r})$ is the spatial density of the positive ions in the arbitrary-shaped nanoparticle with a generally diffuse surface.

Contrary to the Maxwell equations, the hydrodynamic equations (1a)–(1c) are essentially nonlinear. Applying the

perturbation theory with respect to the monochromatic incident laser wave with frequency ω , as well as the steady-state approximation, all the quantities can be expanded into the power series with respect to the incident laser field inside the nanoparticle, which is specified in the dipole approximation by the homogeneous complex fields $\mathbf{E}^L(t)$ and $\mathbf{H}^L(t)$ proportional to $e^{-i\omega t}$. Perturbation expansion of the electron density has the form

$$n_e(t, \mathbf{r}) = n_e^{(0)}(\mathbf{r}) + 2 \text{Re} \sum_{n=1}^{\infty} \sum_{l=0}^n n_e^{(nl)}(\mathbf{r}) e^{-i(n-l)\omega t}, \quad (3)$$

where n marks the order of nonlinearity with respect to the incident field. For a monochromatic external field, each n th-order term can be Fourier expanded. The corresponding summation index is denoted by l , where $0 \leq l \leq n$ for the n th-order term. The same can be written down for all other dynamic quantities, that is, for electron flux density and electron pressure, as well as the self-consistent electric and magnetic fields. For the order n in the laser field nonlinearity, the n th-order harmonic frequency $n\omega$ corresponds to the amplitudes with $l = 0$, but the n th-order lower frequency amplitudes with nonzero $l \leq n$ can also be generally present in Eq. (3) and its analogs for other quantities.

By substituting Eq. (3) and its analogs into Eqs. (1a)–(1c) and collecting the same order of nonlinearity n and the same time dependence $e^{-i(n-l)\omega t}$ simultaneously, a set of equations for the amplitudes with different n and l can be obtained. The amplitudes with $l = 0$ form a closed system of equations, which is independent of the amplitudes with $l \neq 0$. The latter amplitudes describe only higher-order corrections to the main nonlinear contributions. To obtain the system of equations for the main amplitudes with $l = 0$ and with $n \geq 1$, which describe n th-order harmonic generation, it is convenient to rewrite Eqs. (1a)–(1c) and (2a) and (2b) in dimensionless form by introducing new dimensionless variables, namely, $\boldsymbol{\rho} = \mathbf{r}/R_0$, $\mathcal{N}_n = n_e^{(n0)}/(z_i n_{\text{ion}})$, $p_{n\alpha\beta} = P_{\alpha\beta}^{(n0)}/P_0$, and $\mathbf{q}_n = \mathbf{q}^{(n0)}/(z_i n_{\text{ion}} \omega R_0)$, as well as $\mathcal{E}_n = \mathbf{E}^{(n0)}/(4\pi e z_i n_{\text{ion}} R_0)$ and $\mathcal{H}_n = \mathbf{H}^{(n0)}/(4\pi e z_i n_{\text{ion}} R_0)$. The same can be done with the external electric and magnetic laser fields $\mathcal{E}^L(t) \equiv \mathcal{E}_L \mathbf{e}_z e^{-i\omega t} = \mathbf{E}^L(t)/(4\pi e z_i n_{\text{ion}} R_0)$ and $\mathcal{H}^L(t) \equiv -\mathcal{H}_L \mathbf{e}_y e^{-i\omega t} = \mathbf{H}^L(t)/(4\pi e z_i n_{\text{ion}} R_0)$, with $\mathcal{E}_L = E_L/(4\pi e z_i n_{\text{ion}} R_0)$ and $\mathcal{H}_L = \sqrt{\epsilon_1} E_0/(4\pi e z_i n_{\text{ion}} R_0)$. Here, R_0 is the characteristic size of the nanoparticle, P_0 is the characteristic electron pressure, E_0 is the electric field amplitude of the laser wave, and E^L is the external electric field amplitude inside the nanoparticle, which is $(2 + \epsilon_1)E_0/3$ in the spherical approximation.²¹ We assume that the nanoparticle can be surrounded by a dielectric medium with the linear dielectric permittivity ϵ_1 . Then, from Eqs. (1a)–(1c) we obtain the following dimensionless inhomogeneous linear equations for the n th-order quantities:

$$-in\mathcal{N}_n + \text{div } \mathbf{q}_n = 0, \quad (4a)$$

$$\begin{aligned} \mathcal{N}_0^2 \left\{ \left(-in + \frac{\gamma}{\omega} \right) q_{n\alpha} + \frac{A}{\omega^2} \frac{\partial p_{n\alpha\beta}}{\partial \rho_\beta} \right. \\ \left. + \frac{\mathcal{N}_0 (\mathcal{E}_{n\alpha} + \delta_{1n} \mathcal{E}_\alpha^L) + \mathcal{N}_n \mathcal{E}_{0\alpha}}{\omega^2} \right\} = V_{n\alpha}, \end{aligned} \quad (4b)$$

$$\begin{aligned}
& -in\mathcal{N}_0^2 p_{n\alpha\beta} + \mathcal{N}_0 \frac{\partial p_0}{\partial \rho_\gamma} q_{n\gamma} \delta_{\alpha\beta} \\
& + \mathcal{N}_0 p_0 \left(\frac{\partial q_{n\beta}}{\partial \rho_\alpha} + \frac{\partial q_{n\alpha}}{\partial \rho_\beta} + \frac{\partial q_{n\gamma}}{\partial \rho_\gamma} \delta_{\alpha\beta} \right) \\
& - p_0 \left(q_{n\beta} \frac{\partial \mathcal{N}_0}{\partial \rho_\alpha} + q_{n\alpha} \frac{\partial \mathcal{N}_0}{\partial \rho_\beta} + q_{n\gamma} \frac{\partial \mathcal{N}_0}{\partial \rho_\gamma} \delta_{\alpha\beta} \right) = T_{n\alpha\beta}. \quad (4c)
\end{aligned}$$

The dimensionless form of the Maxwell equations inside the nanoparticle is

$$\text{div } \mathcal{E}_n = -\mathcal{N}_n, \quad \text{curl } \mathcal{E}_n = i\tilde{\omega}\tilde{R}_0 \mathcal{H}_n, \quad (5a)$$

$$\text{div } \mathcal{H}_n = 0, \quad \text{curl } \mathcal{H}_n = -\tilde{\omega}\tilde{R}_0 (in\mathcal{E}_n + \mathbf{q}_n). \quad (5b)$$

Here, $\tilde{\omega} = \omega/\omega_p$ is the reduced laser frequency with respect to the plasma frequency, and $\tilde{R}_0 = \omega_p R_0/c$ is the reduced nanoparticle size playing the role of the dipole-approximation parameter. The vector term $V_{n\alpha}$ and the tensor term $T_{n\alpha\beta}$ on the right-hand sides of Eqs. (4b) and (4c), respectively, contain only nonlinear contributions of orders less than n . Therefore, they act as source terms from the lower orders for the n th-order quantities (see details in Ref. 15).

The dimensionless parameter A , which occurs in Eq. (4b), is generally defined as $A = P_0/[4\pi e^2 z_i^2 n_{\text{ion}}^2 R_0^2]$, with P_0 the zero-temperature pressure of the degenerate electron Fermi gas for the current case of cold metal nanoparticles. It can be presented as $A = (l_Q/R_0)^2$, with $l_Q = 3^{1/3}\pi^{1/6}\hbar/[e\sqrt{20m_e}(z_i n_{\text{ion}})^{1/6}]$. Typical values of the quantum length l_Q are in the range of 0.01–0.1 nm. This is smaller than even the minimal possible surface diffuseness, which is of the order of the interatomic distance in metals (about 0.3 nm). It is definitely much smaller than the nanoparticle linear size, which typically is of the order of $R_0 \sim 10$ –100 nm for the subwavelength nanoparticles, which we consider here. Thus, the parameter A is very small, $A \sim 10^{-5}$. Hence, to a first approximation the parameter A can be disregarded. In the case of $A = 0$, the dimensionless static (zeroth-order) equations for the electron density and the electric field inside the nanoparticle have the trivial solution $\mathcal{N}_0(\rho) = n_i(\rho)/n_{\text{ion}}$, $\mathcal{E}_0(\rho) = 0$, if we consider neutral nanoparticles. This means that in this case exact local compensation of positive and negative charges occurs throughout the whole nanoparticle volume. For this reason, the case of $A = 0$ is referred to as the charge compensation approximation (CCA).¹⁵ Note that the CCA is formally equivalent to the approximation of a cold plasma, which is widely used in conventional plasma physics, but in the context of this study the interpretation of the case $A = 0$ as the CCA seems more relevant for the plasma confined in the nanoparticle. It should be noted, however, that in the CCA we obviously ignore the so-called and well-known spill-out effect,^{22,23} which results in a weak redshift of the Mie plasmon resonance in small spherical nanoparticles. However, this effect is really important only for very small nanoparticles with a number of atoms $\lesssim 1000$, and is definitely always small in comparison with modification of the resonance structure of plasmon excitations due to deformation of the surface shape of the nanoparticles which we consider. Also, ignoring spill out we obviously should exclude from general consideration within the CCA some specific cases of nanoparticle surfaces with very sharp concavities and/or convexities, where more sophisticated models should be used.

Equations (4a)–(4c) and (5a) and (5b) constitute the complete set of equations, from which n th-order harmonic generation by the nanoparticle can be determined, at least in principle. They contain the dimensionless parameter \tilde{R}_0 , whose smallness is the criterion of applicability of the dipole approximation. The condition $\tilde{R}_0 \ll 1$ will be used in the solution of these equations for subwavelength nanoparticles. In this case, Maxwell's equations (5a) for the electric field can be approximated by $\text{curl } \mathcal{E}_n = 0$. Hence, the harmonic electric field \mathcal{E}_n can be derived from a potential φ_n , which satisfies the Poisson equation

$$\mathcal{E}_n = -\nabla\varphi_n, \quad \nabla^2\varphi_n = \mathcal{N}_n. \quad (6)$$

The continuity equation (4a), together with the electrostatic equations (6), is equivalent to the equation

$$\mathbf{q}_n + in\mathcal{E}_n = -\text{curl } \mathbf{h}_n. \quad (7)$$

This is just the curl equation from Eqs. (5b), in which the magnetic vector function $\mathbf{h}_n \equiv \mathcal{H}_n/(\tilde{\omega}\tilde{R}_0)$ satisfying the condition $\text{div } \mathbf{h}_n = 0$ should be defined self-consistently.

While solving Eqs. (4b) and (4c), we should discriminate between two cases, $A = 0$ and $A \neq 0$.^{14,15} As mentioned above, we shall consider only the approximation $A = 0$ (the CCA). Then, the term with the electron pressure tensor $p_{n\alpha\beta}$ vanishes in Eq. (4b), and Eq. (4c) becomes superfluous. Hence, with the help of Eq. (4b) the electron flux density \mathbf{q}_n can be explicitly expressed as

$$\mathbf{q}_n = \frac{i\tilde{\omega}^2 \mathbf{V}_n}{\mathcal{N}_0^2(n\tilde{\omega}^2 + i\gamma\tilde{\omega})} + \frac{\mathcal{N}_0(\mathcal{E}_n + \delta_{1n}\mathcal{E}^L) + \mathcal{N}_n\mathcal{E}_0}{i(n\tilde{\omega}^2 + i\gamma\tilde{\omega})}, \quad (8)$$

and using Eq. (7), we obtain the principal equation,

$$\begin{aligned}
& \frac{i(\mathcal{N}_0 - n^2\tilde{\omega}^2 - in\gamma\tilde{\omega})\mathcal{E}_n + i\mathcal{N}_0\delta_{1n}\mathcal{E}^L + i\mathcal{N}_n\mathcal{E}_0}{n\tilde{\omega}^2 + i\gamma\tilde{\omega}} \\
& = \frac{i\tilde{\omega}^2 \mathbf{V}_n}{\mathcal{N}_0^2(n\tilde{\omega}^2 + i\gamma\tilde{\omega})} + \text{curl } \mathbf{h}_n, \quad (9)
\end{aligned}$$

which should be solved together with Eqs. (6), the condition $\text{div } \mathbf{h}_n = 0$, and with the corresponding boundary conditions for the electric potential φ_n and the magnetic vector function \mathbf{h}_n at the nanoparticle surface. If we assume that the nanoparticle is surrounded by a transparent nonmagnetic dielectric, we should introduce the real dielectric permittivities $\epsilon_n \equiv \epsilon(n\omega)$ of the surrounding for different harmonics. For arbitrary-shaped nanoparticles, the first boundary condition at the nanoparticle boundary defined by the condition $\rho = \rho_{\text{lim}}$, with ρ_{lim} dependent on the position on the boundary surface, can be found from the expression for the self-consistent electric potential outside the nanoparticle at $\rho > \rho_{\text{lim}}$:

$$\begin{aligned}
\varphi_n(\rho) &= -\frac{1}{4\pi\epsilon_n} \int d^3\rho' \frac{\mathcal{N}_n(\rho')}{|\rho - \rho'|} = -\frac{1}{4\pi\epsilon_n} \int d^3\rho' \frac{\nabla^2\varphi_n(\rho')}{|\rho - \rho'|} \\
&= \frac{1}{4\pi\epsilon_n} \oint d\mathbf{S}' \left(\varphi_n \frac{\rho - \rho'}{|\rho - \rho'|^3} - \frac{1}{|\rho - \rho'|} \nabla\varphi_n \right). \quad (10)
\end{aligned}$$

Assuming $\rho \rightarrow \rho_{\text{lim}}$ in Eq. (10), where the surface integration should be performed over the nanoparticle boundary, and requiring the continuity of the full electric potential together with the potential of the external laser field on both sides of the nanoparticle surface, we obtain the first boundary condition.

If we set $\rho = \rho_{\text{lim}}$, we should take into account the additional integration in Eq. (10) over an infinitely small hemisphere around the point $\rho = \rho_{\text{lim}}$, and then this boundary condition reads

$$\begin{aligned} & \frac{1}{4\pi\epsilon_n} \oint dS' \left\{ [\varphi_n(\rho') - \varphi_n(\rho)] \frac{\rho - \rho'}{|\rho - \rho'|^3} - \frac{\nabla \varphi_n(\rho')}{|\rho - \rho'|} \right\} \\ & = \varphi_n(\rho) - \delta_{1n} \frac{\epsilon_1 - 1}{\epsilon_1 + 2} (\mathcal{E}^L \cdot \rho). \end{aligned} \quad (11)$$

The other boundary condition corresponds to continuity of the magnetic \mathbf{h}_n function at the nanoparticle boundary. It can be obtained analogously to Eq. (11) and yields

$$\begin{aligned} & \mathbf{h}_n(\rho) + \frac{1}{4\pi} \oint \frac{[(\rho - \rho') \times \{dS' \times [\mathbf{h}_n(\rho') - \mathbf{h}_n(\rho)]\}]}{|\rho - \rho'|^3} \\ & - \oint \frac{[dS' \times \text{curl } \mathbf{h}_n(\rho')]}{4\pi|\rho - \rho'|} - \frac{1}{4\pi} \int d^3\rho' [h_{n\beta}(\rho') - h_{n\beta}(\rho)] \\ & \times \frac{3(\rho - \rho')_\alpha(\rho - \rho')_\beta - \delta_{\alpha\beta}|\rho - \rho'|^2}{|\rho - \rho'|^5} = 0. \end{aligned} \quad (12)$$

However, in this specific form these boundary conditions are applicable only to the nanoparticle with diffuse surface, when all the quantities including the ion density vary smoothly at the nanoparticle surface. In the opposite limiting case of the sharp nanoparticle boundary with the steplike static electron density $\mathcal{N}_0(\rho)$, additional conditions following from Eq. (9) should be taken into consideration to allow for the steplike and higher singularities in the quantities $\nabla \varphi_n$ and $\text{curl } \mathbf{h}_n$ on the sharp nanoparticle surface.

Then, if Eq. (9) is successively solved for all orders in nonlinearity up to n , the nanoparticle dimensionless dipole moment of the n th order in nonlinearity can be calculated as

$$\begin{aligned} \mathbf{d}_n & = - \int \rho \mathcal{N}_n \frac{d^3\rho}{4\pi} = - \int \rho \nabla^2 \varphi_n \frac{d^3\rho}{4\pi} \\ & = \frac{1}{4\pi} \oint \{\varphi_n dS - \rho (dS \cdot \nabla) \varphi_n\}, \end{aligned} \quad (13)$$

where the integration is taken only over the nanoparticle limiting boundary. The higher multipole moments can be expressed in the same vein. They define both the scattering and the absorbing properties of the nanoparticle. For a nanoparticle with an arbitrary shape, we can solve these equations for the laser electric field applied in any direction, if we set $\mathcal{E}^L = \mathcal{E}^L \mathbf{n}$, where \mathbf{n} is the unit vector in the direction of the applied linearly polarized laser field, and \mathcal{E}^L is its module. Then, we can seek the solution of all the equations as expansion in series with respect to the laser electric field module \mathcal{E}^L . In this, however, the solution will generally depend on the laser electric field direction \mathbf{n} .

But even in the case of the CCA, Eq. (9) with the corresponding extra conditions is rather complicated for a general solution, in particular, due to the cumbersome right-hand term with $V_{n\alpha}$ in Eq. (4b) [cf. Ref. 15]. However, at least the problems of low-order (second- and third-order) harmonic generation by the nanoparticle, which is important for various applications can be investigated. Here, to demonstrate the applicability of this approach for the nonspherical case we consider only the linear case of $n = 1$ for perfect cube/parallelepiped like nanoparticles with the steplike surface

as an example, which is of interest in itself and for comparison with the previous approaches such as the DDA, and which will also serve as a first step in solving the nonlinear problems that will be considered elsewhere.

III. LINEAR RESPONSE FOR CUBE-LIKE NANOPARTICLES

In the linear case, from its definition we obviously have $V_1 \equiv 0$. Also, for the neutral nanoparticles in the CCA, the condition $\mathcal{E}_0 = 0$ holds exactly, as was established before. Then, the linear equations read

$$\frac{i(\mathcal{N}_0 - \tilde{\omega}^2 - i\gamma\tilde{\omega})\mathcal{E}_1 + i\mathcal{N}_0\mathcal{E}^L}{\tilde{\omega}^2 + i\gamma\tilde{\omega}} = \text{curl } \mathbf{h}_1, \quad (14a)$$

$$\mathcal{E}_1 = -\nabla\varphi_1, \quad \text{div } \mathbf{h}_1 = 0, \quad (14b)$$

with the expression $\mathcal{N}_1 = \nabla^2\varphi_1$ of the linear approximation for the first-order electron density. Equations (14a) and (14b), as is also the general case of Eq. (9) for arbitrary nonlinearity of the n th order, are four first-order differential equations for four quantities, that is, for three components of the magnetic vector function \mathbf{h}_1 and the scalar potential φ_1 . From these equations the magnetic field $\mathcal{H}_1 = (\tilde{\omega}\tilde{R}_0)\mathbf{h}_1$ neither can be eliminated nor neglected, so even in the dipole approximation $\tilde{\omega}\tilde{R}_0 \ll 1$ all this cannot be reduced to the simpler case of the electrostatic approximation. Being much smaller than the electric field, the magnetic field participates in Eqs. (14a) and (14b) with the electric field on the same footing through the magnetic \mathbf{h}_1 function, and both first-order counterparts of Eqs. (11) and (12) should be used as the boundary conditions to Eqs. (14a) and (14b) to complete their electromagnetic, in essence, solution.

The first-order dipole moment of the nanoparticle with the general surface shape can be written in general tensor form as $d_{1\alpha} = \alpha_{1\alpha\beta}\mathcal{E}_\beta^L$. For a cube, the tensor $\alpha_{1\alpha\beta}$ is diagonal, i.e., $\alpha_{1\alpha\beta} = \alpha_1\delta_{\alpha\beta}$, with α_1 the scalar dipole polarizability. So, for the cubic nanoparticles the dipole moment is always proportional to the applied electric field, $\mathbf{d}_1 = \alpha_1\mathcal{E}^L$. The calculations for the cubic nanoparticle in the linear regime have been performed on the three-dimensional $26 \times 26 \times 26$ cubic grid, where the results were well converged, with the whole cube located at $-0.5 \leq \rho_x, \rho_y, \rho_z \leq 0.5$ (the normalization length R_0 was chosen as the cube edge length: $R_0 = a_x \equiv a_y \equiv a_z$). In this case, the electric potential and three magnetic field components in the cube bulk were given on the cubic grid points themselves, on the vertices of the cubic grid unit cells, while three *outside* surface electric field components were given on the centers of the cubic grid cell faces sited just on the whole cube surface. All these quantities constitute the complete set of variables, which satisfy a closed set of field equations together with the boundary conditions for a perfect cube. In this grid representation, the sharpness of the cube edges and corners is governed only by the cubic grid spacing that is monitored by convergence of the numerical results. The results for the cube scattering and absorption coefficients corresponding to its far-field electromagnetic response that can be expressed through its polarizability α_1 are presented in Figs. 1 and 2. They were checked by fulfillment of the dipole sum rule for the absorption coefficient that follows from the

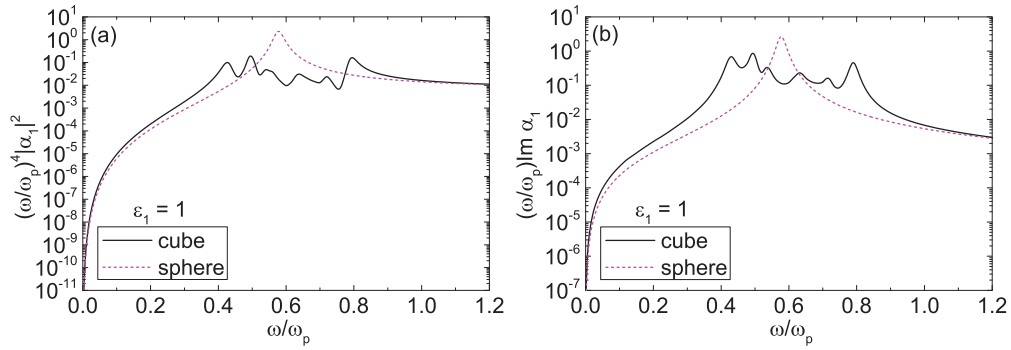


FIG. 1. (Color online) The laser frequency dependence of the normalized linear scattering (a) and absorption (b) coefficients for cubic (solid lines) and spherical (dashed lines) nanoparticles of the same volume in vacuum. The damping constant is $\gamma = 0.03$.

Kramers-Kronig dispersion relations:²¹

$$\int_0^\infty d\omega \omega \text{Im } \alpha_1(\omega) = -\frac{\pi}{2} \lim_{\omega \rightarrow \infty} \omega^2 \text{Re } \alpha_1(\omega) = \frac{1}{8} \frac{3}{2 + \epsilon_1}. \quad (15)$$

It is instructive to compare the cubic nanoparticle with the spherical one of the same volume, with the dimensionless dipole polarizability in vacuum $\alpha_{1 \text{ sphere}}(\tilde{\omega}) = \frac{3}{4\pi} [1 - 3(\tilde{\omega}^2 + i\gamma\tilde{\omega})]^{-1}$ (see Fig. 1). The spherical nanoparticle shows very prominent standard plasmon Mie resonance in both scattering and absorption, which sits at $\omega_p/\sqrt{3} \approx 0.577\omega_p$ in vacuum, and these classical results are precisely reproduced by our model.¹⁵ On a logarithmic scale, the cube nanoparticle demonstrates a quasiplateau behavior of both scattering and absorption in the frequency range of the spherical Mie resonance,

as compared with the corresponding results for the spherical particle. The Mie plasmon resonance is redshifted in the surrounding medium with increasing dielectric permittivity ϵ_1 proportional to $\epsilon_1^{-1/2}$,¹⁵ and this universal behavior is also seen for the cubic nanoparticles (see Fig. 2). In a normal scale, we see that our calculations of the linear scattering and absorption coefficients of a cubic nanoparticle are qualitatively close to, but quantitatively somewhat different from those of prior authors mainly using the DDA method.^{2,9,11–13} In vacuum, the frequency dependence of both scattering and absorption coefficients displays six peaks, from which there are three dominant peaks located approximately at $0.43\omega_p$, $0.49\omega_p$, and $0.79\omega_p$. Note that the first two close low-frequency peaks, especially for a cube in a dielectric environment, can be qualitatively interpreted as a single double-split resonance mode. Our results reproduce well the global structure of six resonances that were first obtained in Refs. 2 and 9,

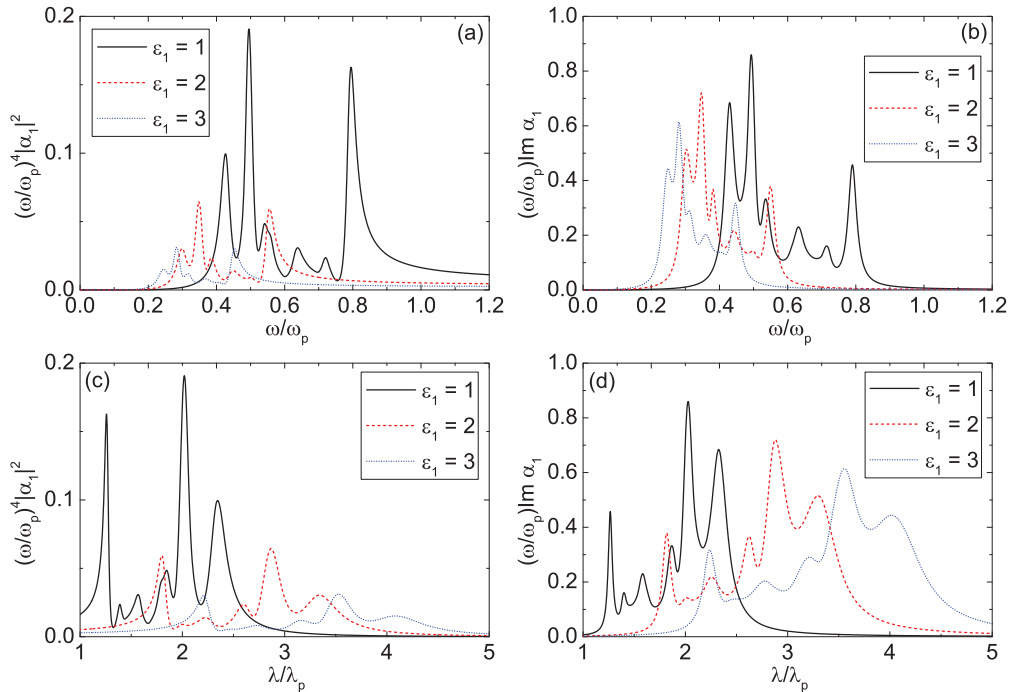


FIG. 2. (Color online) The laser frequency [(a) and (b)] and laser wavelength [(c) and (d)] dependence of the normalized linear scattering [(a) and (c)] and absorption [(b) and (d)] coefficients for cubic nanoparticles at different dielectric surrounding permittivities $\epsilon_1 = 1$ (solid lines), $\epsilon_1 = 2$ (dashed lines), and $\epsilon_1 = 3$ (dotted lines). The damping constant is $\gamma = 0.03$.

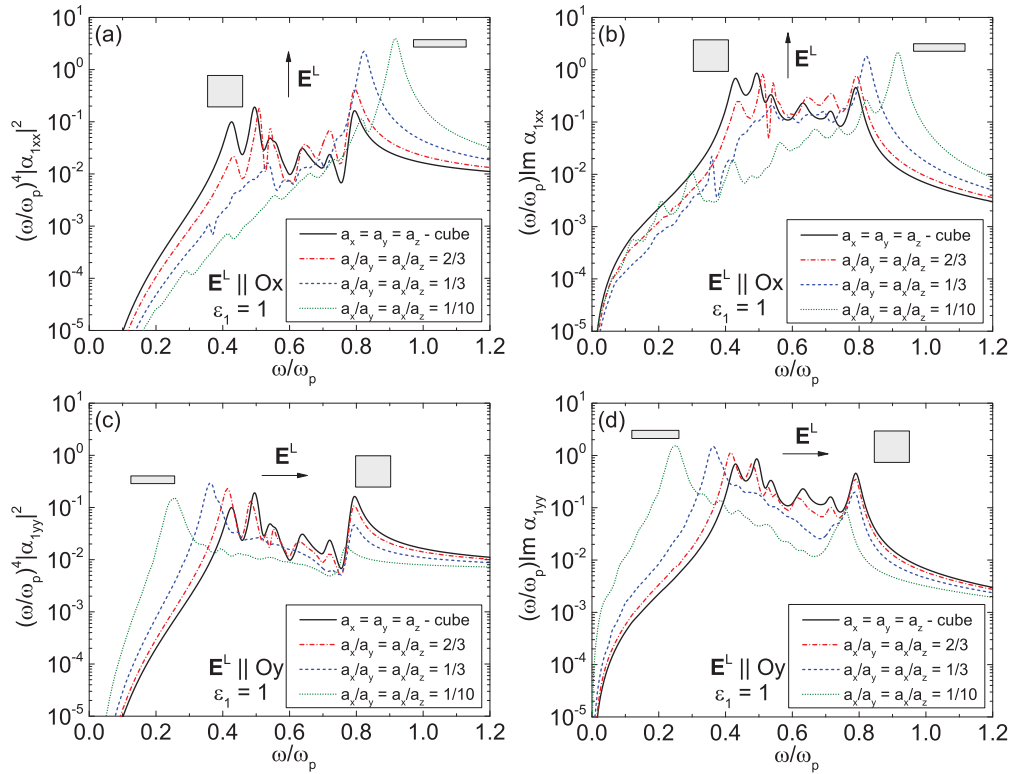


FIG. 3. (Color online) The laser frequency dependence of the normalized linear scattering [(a) and (c)] and absorption [(b) and (d)] coefficients in vacuum for nanoparticles in the form of cube (solid lines) and rectangular parallelepipeds of the same volume (dash-dotted, dashed, and dotted lines) for different ratios $a_x/a_y \equiv a_x/a_z$ for their sides. In the panels (a) and (b) the laser field is directed along the x axis associated with the shortest dimension, while for panels (c) and (d) the laser field is directed along the y axis associated with the long dimension of the square parallelepiped. The damping constant is $\gamma = 0.03$. The gray blocks mark the main pick for a cubic particle (square) and thin slab (rectangle).

although some resonance positions and the relative strengths are quantitatively different. It concerns especially the position of the higher-frequency resonance, which is at $0.79\omega_p$ in the current paper, and with the relative strength of two neighboring dominant low-frequency resonances. But our results presented as a function of laser wavelength $\lambda = 2\pi c/\omega$ in Figs. 2(c) and 2(d) are in a very good agreement with the results for a cube presented in Ref. 11. Also, there is a qualitative agreement with the results presented in Refs. 12 and 13 in the restricted wavelength range of 300–500 nm for different smoothed silver cubes, where, however, only one dominant peak with the single low-wavelength/high-frequency satellite is present even for a perfect cube. It corresponds to our results in Fig. 2(d) for laser absorption in the range around $\lambda/\lambda_p = 2$, with $\lambda_p \equiv 2\pi c/\omega_p$, corresponding to the central dominant peak with the single short-wavelength satellite, too. However, the right long-wavelength resonance presented in our results in Fig. 2(d) for laser absorption, as well as in the results of Refs. 2 and 11, is not seen in the results of Ref. 13. The reasons for this could be either a restricted range of wavelength where these results are presented, with a loss of this long-wavelength resonance, or merging of two right dominant resonances in a single one in a still imperfect cube, due to smoothing of the cube edges and corners. In any case, the latter reason can be applied to the similar corresponding experimental results presented also in Ref. 13. However, we would like to also stress

that our results can be directly applied only to nanoparticles of simple metals with well-defined plasma frequency ω_p , while for noble metals such as silver or gold due to deviations from the simple Drude models it should be partially modified in order to account for different roles of s electrons and d electrons, as well as the interband transitions.^{24,25}

For an additional check of our results, and also for a deeper understanding of the origin of these resonance peaks in the scattering and absorption dispersion curves of the cube nanoparticle, we have also carried out calculations of the polarizability of rectangular parallelepipeds of the same volume, but with the shorter edge size a_x along the x axis, which is reduced with respect to the other two equal edge sizes ($a_y = a_z$) with the coefficients 2/3, 1/3, and 1/10, respectively. In this case, we should discriminate between the polarizability tensor components α_{1xx} and $\alpha_{1yy} \equiv \alpha_{1zz}$. The results for the corresponding scattering and absorption coefficients in vacuum are shown in Fig. 3 along with the results for an ideal cube. From Figs. 3(a) and 3(b), it is clearly seen that the cubic plasmon resonance with the highest frequency $0.79\omega_p$ is a direct descendant of the single dominant plasmon resonance just near the plasma frequency in a thin metal plate, when the laser electric field is directed along the x axis, perpendicularly to the plate. This is not unexpected, because transformation of a sphere to a cube makes it closer to a slab, for which the resonance frequency in the perpendicular

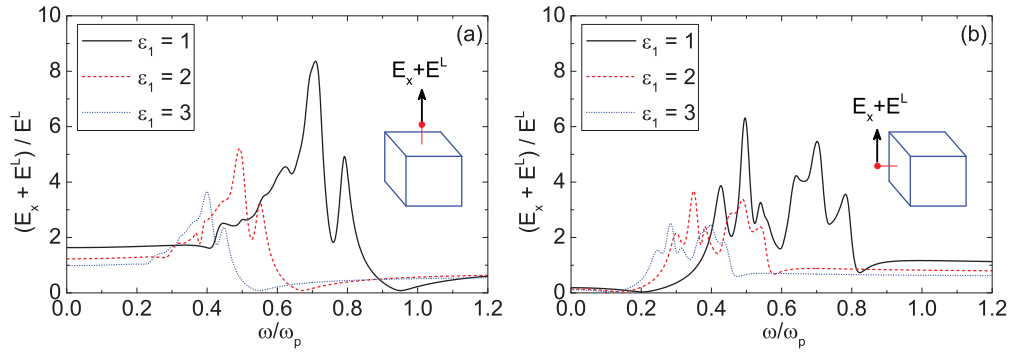


FIG. 4. (Color online) The laser frequency dependence of the normalized amplitudes of the total electric field directed along the laser electric field: (a) just above the center of the cube face (at $\rho_x = 0.6$, $\rho_y = \rho_z = 0$) oriented perpendicularly to the laser electric field directed along the x axis and (b) just above the center of the cube face (at $\rho_y = -0.6$, $\rho_x = \rho_z = 0$) oriented parallel to the laser electric field. The permittivities of the dielectric surrounding are $\epsilon_1 = 1$ (solid lines), $\epsilon_1 = 2$ (dashed lines), and $\epsilon_1 = 3$ (dotted lines). The damping constant is $\gamma = 0.03$.

direction is just the plasma frequency ω_p ,¹⁴ so the intermediate position of this high-frequency resonance for the cube between those for the sphere and the slab is rather natural. On the other hand, the results presented in Figs. 3(c) and 3(d) show that the cubic plasmon resonance with the lowest frequency $0.43\omega_p$ is a descendant of the low-frequency plasmon resonance in a slab, in the case when the laser electric field is directed along the y axis parallel to the slab. In the same vein, one may suppose that the central dominant resonance of a cube nanoparticle at $0.49\omega_p$ is a direct descendant of the plasmon Mie resonance in a sphere, which is strongly redshifted from the position for a sphere at $\approx 0.577\omega_p$. Note that this point of view is well supported by calculations of this plasmon resonance by the DDA in Refs. 11 and 13 for cubes with smoothed edges and corners, when the resonance gradually loses its satellites, increases in amplitude, and is simultaneously shifted to lower wavelengths with increased edge smoothness.

For a cube, we have also inspected the near-electric-field resonance behavior just above the two different cube faces in its centers (see Fig. 4), as well as just near the vertex of the cube along the cube diagonal (see Fig. 5). It appears that the resonance behavior of the total electric field in all these points is quite different. While the almost single dominant resonance peak in the total electric field near the cube face

perpendicular to the applied laser electric field is located in vacuum at high frequency $\approx 0.71\omega_p$ [together with the only close weaker satellite at $\approx 0.79\omega_p$; see Fig. 4 (a)], several resonances in a wide range of frequencies are present in the total electric field near the cube face parallel to the applied laser electric field [see Fig. 4(b)].

On the other hand, the position of the single dominant resonance in the total electric field near the cube vertex, for all its components, is located in vacuum at $\approx 0.43\omega_p$, which is in the range of low-frequency plasmon resonance (cf. Fig. 5 with Fig. 4). All this supports the view that the cube can be considered as an intermediate shape between a sphere and a slab. The considerable difference in the resonant behavior of the electric near field in the different points near the nanoparticle surface (for example, near the different cube faces in its centers, and near the cube vertices) can be important for the different nanoplasmonics applications.

IV. CONCLUSION

In summary, the self-consistent hydrodynamic plus electrodynamic model has been developed for plasmon excitations in metal nanoparticles with general nonspherical shapes in the dipole approximation. In addition, the model allows one

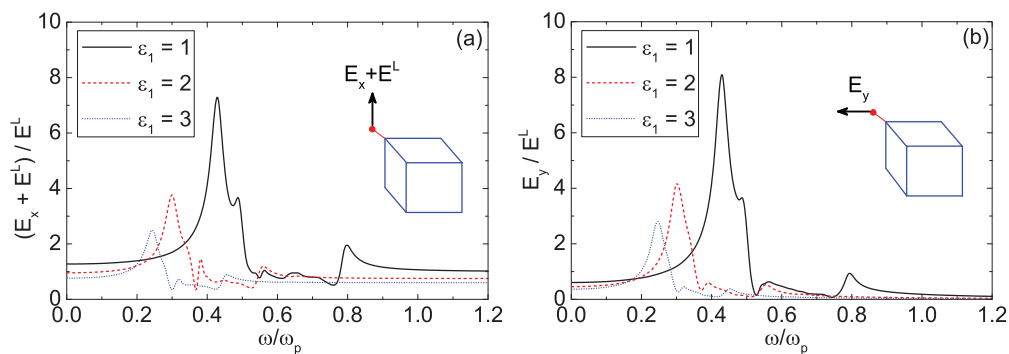


FIG. 5. (Color online) The laser frequency dependence of the normalized amplitudes of the total electric field components just near the vertex of the cube along the cube diagonal (at $\rho_x = \rho_z = 0.558$, $\rho_y = -0.558$): (a) along the laser electric field directed along the x axis and (b) perpendicularly to the laser electric field (along the y axis). The permittivities of the surrounding dielectric are $\epsilon_1 = 1$ (solid lines), $\epsilon_1 = 2$ (dashed lines), and $\epsilon_1 = 3$ (dotted lines). The damping constant is $\gamma = 0.03$.

to consider both linear and nonlinear plasmon excitations in such nanoparticles. Importantly, the magnetic field is involved in the theory on the same footing as the electric field even for subwavelength nanoparticles in the dipole approximation. The diffusive surface was incorporated into the theory, which is decisively important for the nonlinear plasmon excitation in the charge compensation approximation. In the current paper, the model was first applied to cubic and rectangular parallelepiped

nanoparticles in the linear regime, and a comparison with other approaches such as the DDA developed earlier has been performed. As a proof of concept, we have shown that the linear regime is well described by the present method, and this opens up the possibility of calculating the linear, as well as the nonlinear responses of cubelike and more complex nanoparticles and their assemblies that will be addressed elsewhere.

*fomichev@imp.kiae.ru

†alex.bratkovski@gmail.com

¹S. A. Maier, *Plasmonics: Fundamentals and Applications* (Springer, New York, 2007).

²R. Ruppin, *Z. Phys. D* **36**, 69 (1996).

³F. S. Ou, M. Hu, I. Naumov, A. Kim, W. Wu, A. M. Bratkovsky, X. Li, R. S. Williams, and Z. Li, *Nano Lett.* **11**, 2538 (2011).

⁴S. Kim, J. Jin, Y.-J. Kim, I.-Y. Park, Y. Kim, and S.-W. Kim, *Nature (London)* **453**, 757 (2008).

⁵M. Kauranen and A. V. Zayats, *Nat. Photonics* **6**, 737 (2012).

⁶I. D. Mayergoyz, D. R. Fredkin, and Z. Zhang, *Phys. Rev. B* **72**, 155412 (2005).

⁷U. Hohenester and J. Krenn, *Phys. Rev. B* **72**, 195429 (2005).

⁸E. M. Purcell and C. P. Pennypacker, *Astrophys. J.* **186**, 705 (1973).

⁹R. Fuchs, *Phys. Rev. B* **11**, 1732 (1975).

¹⁰G. C. Schatz, *J. Mol. Struct.: THEOCHEM* **573**, 73 (2001).

¹¹C. Noguez, *J. Phys. Chem. C* **111**, 3806 (2007).

¹²C. M. Cobley, S. E. Skrabalak, D. J. Campbell, and Y. Xia, *Plasmonics* **4**, 171 (2009).

¹³N. Grillet, D. Manchon, F. Bertorelle, C. Bonnet, M. Broyer, E. Cottancin, J. Lermé, M. Hillenkamp, and M. Pellarin, *ACS Nano* **5**, 9450 (2011).

¹⁴S. V. Fomichev, D. F. Zaretsky, and W. Becker, *Phys. Rev. B* **79**, 085431 (2009).

¹⁵S. V. Fomichev and W. Becker, *Phys. Rev. A* **81**, 063201 (2010).

¹⁶S. V. Fomichev, S. V. Popruzhenko, D. F. Zaretsky, and W. Becker, *J. Phys. B: At. Mol. Opt. Phys.* **36**, 3817 (2003).

¹⁷S. V. Fomichev, S. V. Popruzhenko, D. F. Zaretsky, and W. Becker, *Opt. Express* **11**, 2433 (2003).

¹⁸G. Y. Panasyuk, J. C. Schotland, and V. A. Markel, *Phys. Rev. Lett.* **100**, 047402 (2008).

¹⁹A. A. Gomyadinov, G. Y. Panasyuk, J. C. Schotland, and V. A. Markel, *Phys. Rev. B* **84**, 155461 (2011).

²⁰E. M. Lifshitz and L. P. Pitaevskii, *Physical Kinetics* (Pergamon, Oxford, 1981).

²¹L. D. Landau and E. M. Lifshitz, *Electrodynamics of Continuous Media* (Pergamon, Oxford, 1984).

²²V. V. Kresin, *Phys. Lett. A* **133**, 89 (1988).

²³G. Weick, G.-L. Ingold, R. A. Jalabert, and D. Weinmann, *Phys. Rev. B* **74**, 165421 (2006).

²⁴V. V. Kresin, *Phys. Rev. B* **51**, 1844 (1995).

²⁵U. Kreibig and M. Vollmer, *Optical Properties of Metal Clusters* (Springer, Berlin, Heidelberg, 1995).